electronics

MDPI

Article

Power Quality Assessment of Grid-Connected PV System in Compliance with the Recent Integration Requirements

Ali Q. Al-Shetwi [1,2], M A Hannan [2,*], Ker Pin Jern [2], Ammar A. Alkahtani [1] and A. E. PG Abas [3]

1 Institute of Sustainable Energy, University Tenaga Nasional, Kajang 43000, Malaysia; ali.qasem@uniten.edu.my (A.Q.A.-S.); Ammar@uniten.edu.my (A.A.A.)
2 Department of Electrical Power Engineering, University Tenaga Nasional, Kajang 43000, Malaysia; pinjern@uniten.edu.my
3 Faculty of Integrated Technologies, Universiti Brunei Darussalam, Gadong BE1410, Brunei; emeroylariffion.abas@ubd.edu.bn
* Correspondence: hannan@uniten.edu.my; Tel.: +603-89217257

Received: 10 December 2019; Accepted: 9 January 2020; Published: 21 February 2020

Abstract: The generation and integration of photovoltaic power plants (PVPPs) into the utility grid have increased dramatically over the past two decades. In this sense, and to ensure a high quality of the PVPPs generated power as well as a contribution on the power system security and stability, some of the new power quality requirements imposed by different grid codes and standards in order to regulate the installation of PVPPs and ensure the grid stability. This study aims to investigate the recent integration requirements including voltage sag, voltage flicker, harmonics, voltage unbalance, and frequency variation. Additionally, compliance controls and methods to fulfill these requirements are developed. In line with this, a large-scale three-phase grid-connected PVPP is designed. A modified inverter controller without the use of any extra device is designed to mitigate the sage incidence and achieve the low-voltage ride-through requirement. It can efficiently operate at normal conditions and once sag or faults are detected, it can change the mode of operation and inject a reactive current based on the sag depth. A dynamic voltage regulator and its controller are also designed to control the voltage flicker, fluctuation, and unbalance at the point of common coupling between the PVPP and the grid. The voltage and current harmonics are reduced below the specified limits using proper design and a RLC filter. The obtained results show that the proposed controller fulfilled the recent standard requirements in mitigating power quality (PQ) events. Thus, this study can increase the effort towards the development of smooth PVPP integration by optimizing the design, operation and control strategies towards high PQ and green electricity.

Keywords: grid-connected PV system; power quality; renewables integration; low voltage ride through; technical requirements; grid code

1. Introduction

Over recent years, the production and installation of photovoltaic power plants (PVPPs) have seen a huge increase all over the world. The level of penetration continues to grow, with approximately 100 GW of generated power has been added last year only, which makes photovoltaic (PV) systems contribute to about 55% of the newly added renewable energy capacity across the globe. This high growth of PVPPs generation and integration is anticipated to be maintained in the future. Figure 1 illustrates the amount of PV system capacity and annual addition in the recent ten years [1]. PVPPs have various characteristics that differ from the traditional power plants, which in turn lead to new

challenges for grid-connected PV systems (GCPS). Moreover, the high penetration of this renewable power source starts to affect the stability, security, reliability, and quality of the power system. Voltage fluctuation, voltage sag, harmonics, voltage flicker, power factor, and voltage unbalance at the point of common coupling (PCC) can lead to a negative impact on the power network and thus should be addressed. For this, the grid codes of many countries and other international standards are imposing some new and stringent technical requirements concerning the integration of PVPPs into the utility grid. These technical requirements are enforced to guarantee that no bad quality of power would be injected into the grid. Furthermore, PVPPs are required to behave like traditional power plants and support the grid during disturbances [2].

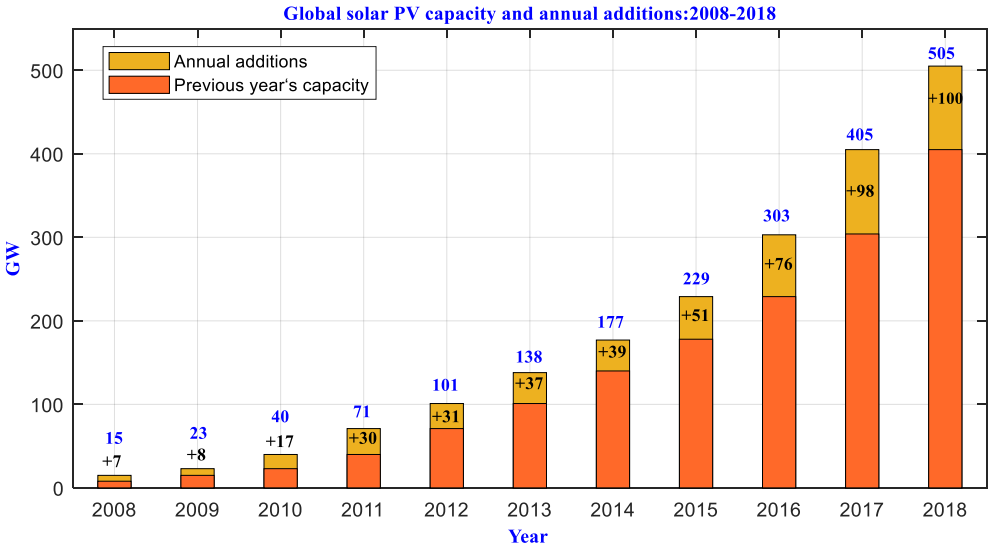

Figure 1. Photovoltaic (PV) capacity and annual addition in the last ten year.

For power quality, grid codes from countries such as Germany [3], Italy [4], USA [5], Australia [6], and many international standards like IEC standards [7] and IEEE standards [8] have enforced strict power quality rules for PV and other renewable energy sources (RESs) integration. For instance, during voltage sag, which is normally caused by the grid faults, the new requirements necessitate injecting reactive current into the PV system to overcome the sag event and to support the grid stability [9,10]. The limits of voltage fluctuation, harmonics, power factor, voltage unbalance, and flicker have also been defined and imposed. Different countries have set their own rules, requirements, and standards as summarized in [9,11–14]. However, verification and implementation can be more important than setting rules and regulations. Some recent studies have been conducted as an effort to apply these requirements for GCPS, especially power quality issues due to the proliferation of highly sensitive electronic equipment [15]. In this regard, a study proposed in [16,17] used the static synchronous compensator (STATCOM) in order to mitigate the sag event and meet the low voltage ride-through (LVRT) requirements. The Static var compensator (SVC) [18] and energy storage system [19] are presented to fulfill the LVRT and inject reactive current to support the grid and overcome the sag incident as well. D-STATCOM also was used to mitigate the harmonics at the point of common coupling between the PVPP and the main grid [20]. The studies mentioned above have achieved quite significant results; however, most of these techniques are costly and can increase system complexity. In addition, some of these studies did not address the power balance and the protection of the semiconductor device during sag. Furthermore, attempts are yet to be made to study the effect of voltage unbalance and flicker regarding PV system penetration. For instance, the study proposed in [21,22] addressed voltage unbalance problem and the flicker issue was addressed by [23]. However, these phenomena were not investigated sufficiently and the standards and requirements were not considered.

This study aims to design a 5 MW large-scale PVPP connected to the medium voltage (MV) side of the grid according to the recent standard requirements. The paper mainly focuses on the assessment and management of the power quality issues to be fulfilled at the PCC as imposed by the new standards. This includes studying voltage sag, fluctuation, flicker, unbalance as well as current and voltage harmonic distortion, frequency behavior, and power factor to perform a comprehensive assessment of the PQ problems on the large-scale PV system based on the standard requirements. The main novelties and contributions are as follows:

- A comprehensive control strategy that enables the PVPP to withstand grid faults, allow the inverter remains connected, continuously produce electricity, and absorb excessive energy whilst injecting the required reactive power to meet the LVRT requirements and overcoming sag event. This controller can inject active and reactive current during the fault without any extra hardware in compare to STATCOM, SVC, or energy storage system (ESS), which means less complexity and lower cost.
- An advanced dynamic voltage regulator (DVR) control system to reduce the voltage fluctuation, flicker, and unbalance into the required limits efficiently. The main feature of the proposed controller to address the flicker incident is injecting voltages in sequence into the power line at PCC using DVR three-phase voltage source inverter. A fast and precise detection method based on the voltage phage angle in a balanced situation is proposed to detect the unbalance so that it can overcome the balance incident based on mathematical modeling is developed.
- An efficient RLC filter to reduce the voltage and current harmonics under the specified limits at the increased switching frequency is developed.

These advanced features are managed to achieve the desired level of PQ issues at the PCC as imposed by the new standards. Accordingly, the simulation results showed that all the power quality issues are modified and degrade to the standard defined level using efficient controls and compliance strategies.

2. The Recent PV Integration Requirements

The installation of the PVPPs comes along with many challenges that need to be addressed before they can be incorporated into the utility grid. This is because the operation of these plants can be uncertain due to the variability of the solar. It is important to investigate the establishment of grid codes for the installation of PVPPs and how they can help to achieve reliable operation and long-life production. The effect of high PVPPs connection to the existing power grid should be evaluated in terms of the power flow patterns to ensure a high quality of the delivered power and overall system reliability and stability. In this regard, and due to the slow replacement of RESs such as PV system to the conventional generation units, the power system operators (PSOs) have issued strict technical requirements concerning this connection that must be achieved at the PCC to ensure robust operation and good quality of the power future. The following subsection provides a brief overview of the recent integration requirements.

2.1. LVRT Capability Requirement toward Voltage Sag Mitigation

Voltage sag (dip) is undoubtedly one of the most severe power quality problems in the power industry as well as to commercial and industrial customers. The sag incident in power networks leads to grid stability problems. It is mainly caused by grid faults and is defined as the deviation of RMS voltage between 10% and 90% of its nominal value during short period of time [24]. In the past, during sag events, standard requirements necessitate that the PVPPs have to disconnect from the grid quickly to prevent islanding issues. However, as the penetration of PVPPs to the power grid rises, its disconnections during sags are unfavorable. This is because it can cause a huge loss of the PV-generated power, which in turn leads to problems in the operation and stability of the grid [25].

Accordingly, the low voltage rise-though (LVRT) capability is enforced by recent requirements to help in solving the sag problems and contribute to grid stability [26].

The LVRT is defined by the modern standard and grid codes (GCs) as the ability of the PVPP to stay in connection mode during voltage sag for a specific duration and support the voltage recovery until it overcomes the sag event. The typical LVRT standard requirements are similar to Figure 2a. Thus, in case the voltage level is in area A, the PVPP should resist the sag fault and operate regularly for a period ranging from t_0 to t_1; otherwise, the disconnection is mandatory. If the voltage at PCC is varying in area B and retrieved after sag event to V_x within t_2, it is compulsory for the PVPP to stay in operation without the trip. It is also important to mention that the values of V_x, V_y, V_0, t_0, t_1, and t_2 are differing from country to country [27,28]. Not only to withstand the fault but also to inject reactive current based on the voltage drop according to the curve shown in Figure 2b is also an advance LVRT requirement to mitigate voltage sag. Accordingly, in case the voltage above 90%, no injection of reactive current, however, if the fault caused the voltage to drop between 90% and 50% (area A), the PVPP must support the voltage stability and mitigate the voltage sag by injection of amount of reactive current depend on the curve provided. To overcome sag events during the worst case (B area) once the voltage dropped to less than 50%, the grid voltage recovery must be supported by injection at least 100% of the available reactive current [9].

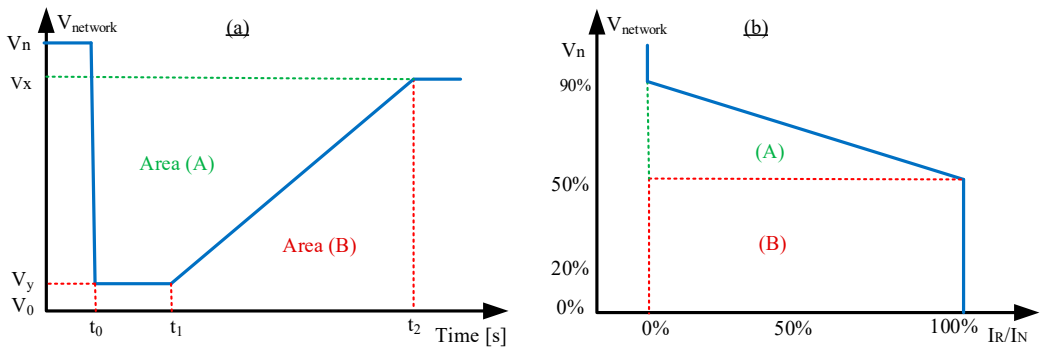

Figure 2. Low voltage ride-through (LVRT) requirements during voltage sag: (**a**) general curve limits and (**b**) reactive current support.

2.2. Voltage Flicker Requirements

The power output from PVPP is highly sporadic, accordingly, generating a different amount of voltage flickers and voltage variance on the distribution networks. The flicker can occur as possible effects that PV systems penetration into the power system caused due to the variations in solar irradiance. In this regard, the flicker assessment and management have gained more concern recently and have been imposed on power quality requirements for distribution systems generation. The measurement of flicker is given by the short term probability flicker severity (P_{st}) and the long term probability flicker severity (P_{lt}) based on the calculation mentioned in [29].

To measure the P_{st} and P_{lt}, IEC standard 61000-4-15, defines the measuring time should be at least lasting for ten minutes and 2 h, respectively [30]. The Canadian CSA C22.3 No. 9-08 [31] and IEEE 1547 [8] standards require that the distribution source shall not create objectionable flicker between 0.6 and 0.9 pu for P_{lt} and P_{st}, respectively. Additionally, IEEE 929, IEEE 519, and IEC 61727 state that PVPP integrated power grid should not exceed the limit specified in IEC standard 61000-4-15 [30]. The voltage flicker requirements for GCPs in China's GB and Taiwan's CNS standards stated that the PVPP should not produce short and long term flicker above the limits specified by IEC. UK-EREC G83 standards state that the long- and short-term flicker shall not exceed 0.65 and 1.0, respectively. Overall, Table 1 lists the long- and short-term flicker limits stated by different countries grid codes and standards. Thus, an advanced controller with flicker mitigating device is important in compliance with grid features.

Table 1. Voltage flicker limits at different voltage levels.

The Standards	Network	P_{lt}	P_{st}
IEEE Std. 1547	MV	0.7	0.9
	HV-EHV	0.6	0.8
UK	MV-HV	0.65	1.0
IEC61000	MV	0.8	1.0
Malaysian GC	LV (less than 11 kV)	0.8	1.0
	MV (11–33) kV	0.7	0.9
	HV (above 33 kV)	0.6	0.8
USA	LV	0.7	0.9
	MV-HV	0.6	0.8
Brazil	LV-MV	0.8	1.0
Jordan (FICHTNER)	MV-LV	0.46	1.0

2.3. Requirements of PV Harmonics Distortion

Harmonic distortion is defined as the voltage and current waveform distortion, which causes it to change from its normal characteristics or shape. It is generally classified as a serious power quality problem. In the PV system, the harmonics can be produced due to the use of inverter, converter, and other power electronic devices. In this context, the PVPP contains several power-electronic devices that produce distortion [32]. Furthermore, the amplitudes of high current and voltage harmonic make additional losses in the power grid and malfunctioning of grid-side protection devices. Therefore, strict regulation is imposed to ensure a less level of harmonic distortion at the PCC. The harmonic distortion can be characterized and measured by total harmonic distortion (THD) of either voltage or current as expressed in [33].

During the advancement of the PV system integration requirements into the grid, different harmonic distortion standards are imposed; however, they are similar, excluding EREC G83 and VDE-AR-N4105, which are notably strict in which imposed a THD for PV integration should be less than 3% [34,35]. Tables 2 and 3 provide the harmonic limits that should be achieved at PCC for current and voltage, respectively.

Table 2. Current harmonics distortion limits of the PV systems.

The Standards	Type	Harmonic Order (h)	Distortion Limit	THD (%)
IEEE 1547 AS 4777.2 (Australia), GB/T (China), and ECM (Malaysia)	Odd	33 < h	<0.3%	<5%
		23 ≤ h ≤ 33	<0.6%	
		17 ≤ h ≤ 21	<1.5%	
		11 ≤ h ≤ 15	<2%	
		3 ≤ h ≤ 9	<4%	
	Even	10 ≤ h ≤ 32	<0.5%	
		2 ≤ h ≤ 8	<1%	
UK (EREC G83 Stds.)	Odd	h = 3, 5, and 7	<(2.3, 1.14, and 0.77)%	<3%
		h = 9, 11, and 13	<(0.4, 0.33, and 0.21)%	
		11 ≤ h ≤ 15	<0.15%	
	Even	h= 2, 4, and 6	<(1.08, 0.43, and 0.3)%	
		8 ≤ h ≤ 40	<0.23%	
IEC 61000-3-2	Odd	h = 3, 5, and 7	<(3.45, 1.71, and 1.15)%	<5%
		h = 9, 11, and 13	<(0.6, 0.5, and 0.3)%	
		15 ≤ h ≤ 39	<0.225%	
	Even	h = 2, 4, and 6	<(1.6, 0.65, and 0.45)%	
		8 ≤ h ≤ 40	<0.345%	

Table 3. Voltage harmonics distortion limits of the PV systems.

The Standards	Voltage Bus	Max. Individual Harmonics	THD (%)
IEEE 519	(V ≤ 1) kV	5%	8%
	(1 ≤ V ≤ 69) kV	3%	5%
	(69 ≤ V ≤ 161) kV	1.5%	2.5%
	(V > 161) kV	1%	1.5%
IEC 61000-3-2	(2.3 ≤ V ≤ 69) kV	3%	5%
	(69 ≤ V ≤ 161) kV	1.5%	2.5%
	(V > 161) kV	1%	1.5%

2.4. Standard Requirement for Voltage Unbalance

A voltage unbalance or imbalance occurs in the electrical system when the line voltage or phase varies from the typical balance condition. Despite there are different reasons that may contribute to voltage unbalance, the voltage unbalance may happen in supply systems [36]. Additionally, from the power quality and reliability view, having a worthy voltage balance in the power grid is paramount. Thus, to ensure a smooth interconnection of the PVPP with voltage balance, some GCs and standards requirements have been imposed. The degree of voltage unbalances commonly defined as the ratio of positive to negative sequence voltage component. In this regard, the voltage unbalance factor (VUF) is used to monitor the degree of unbalance as mentioned in [37].

As the unbalance of voltage is a good indicator of the quality of power delivered to the grid, some standards and GCs take attention to limits the VUF at PCC and then ensure that non-unbalance three-phase voltage is injected into the grid. For instance, IEEE Std. [8] requires VUF not exceed 3%. IEC standard imposed that all distribution generators have to keep the VUF less than 2% [38]. German and China requirements have imposed 2% of voltage unbalance at the interconnection point of PVPP with electrical grid [3,39,40]. In Canada, CAN/CSA-C61000-2-2 standard required that the maximum limit for voltage unbalance is 2%, however, 3% is allowed in case of unbalanced loading as mentioned by Canadian standards association [31]. Overall, the standards across the globe have specified the suitable limit for voltage unbalance to generally varying between 1% and 2% [39,41] should not be exceeded.

2.5. PV System Requirements on Frequency Variation and Power Factor

The response of PVPPs to the grid frequency variation standards are thoroughly highlighted during the last years as the frequency consider one of the key factors to ensure a high quality of the power systems. Therefore, some recent requirements impose the PV system to work under frequency control in which operates at a nominal frequency (i.e., 50 or 60 Hz) with a specified margin; otherwise, speedily disconnection is required. Normally, this margin is determined by ±1 Hz as specified by many regulations [42]. Thus, the frequency is not allowed to fluctuate less than 1 Hz. The efficient use of electricity indicated by the power factor, which is estimated on a scope of 0–1.0. In the power system, as all circuits include inductance and capacitance to a specific degree, the power factor practically is always under one. Table 4 lists the minimum power factor limit in various grid codes regarding the PVPPs integration that should be achieved at the connection point.

Table 4. Power factor range at point of common coupling (PCC) in different grid codes.

Requested By	Power Factor Range Point of Common Coupling	
	Lead	Lag
Germany	0.95	0.95
Italy	0.90	0.90
China (GB/T)	0.95	0.95
Spain	0.85	0.85
Australia	0.9	0.95
South Africa	0.95	0.95
Belgian regulation C10/11	0.95	0.95

3. Grid-Connected PV System Structure and Models

A single-stage three-phase GCPS is designed and simulated in this study. It mostly consists of PV array, MPPT controller, inverter, controller, filter, transformer, and grid, as illustrated in Figure 3. The PV modules are arranged in series and parallel to configure the array system so that it can be delivered the required DC-voltage to the DC side of the inverter. The DC power then converted to AC power via the inverter, and eventually filtered, transformed, and integrated to the required level of the grid side. A single-stage GCPS has only DC/AC energy conversion, which has different advantages such as high efficiency, simple structure, robust flexibility, and low system cost. In this model, the centralized conversion system in which the PV array system is connected to one central inverter is designed.

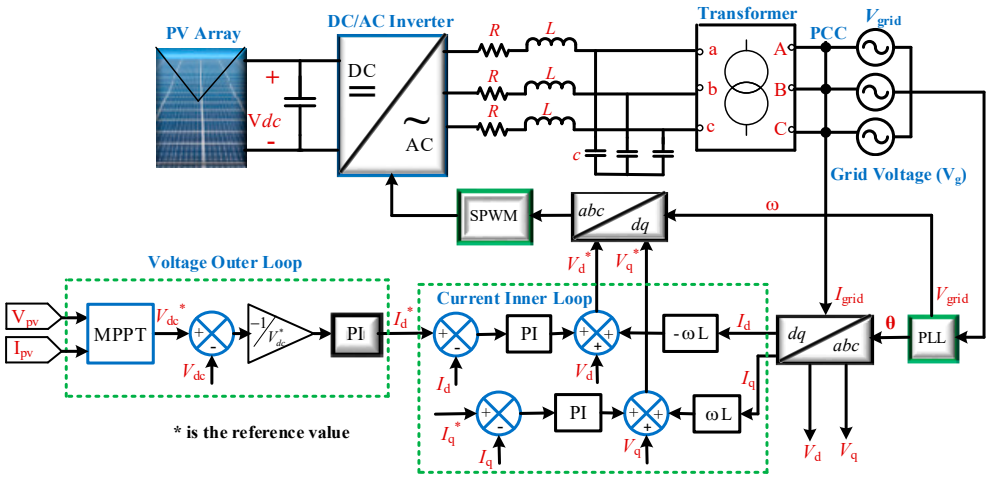

Figure 3. The overall structure of the single-stage PV power plant connected grid.

However, the complexity is high because the inverter has to achieve all control objectives alone. Figure 4 shows the three-phase view of the grid-connected inverter. The inverter voltage equations when considering the access to the utility grid based on Figure 4, are driven as follows:

$$V_{ia} = Ri_a + L\frac{di_a}{dt} + V_{ga}, V_{ib} = Ri_b + L\frac{di_b}{dt} + V_{gb}, \text{ and } V_{ic} = Ri_c + L\frac{di_c}{dt} + V_{gc}, \quad (1)$$

where (V_{ga}, V_{gb}, V_{gc},), (V_{ia}, V_{ib}, V_{ic}), and (i_a, i_b, i_c) represent three-phase (3-ph) voltage of the grid, (3-ph) voltage of the inverter, and (3-ph) current in the inverter, respectively. The mathematical formulation of the grid inverter in the *d*–*q* synchronous frame at a line frequency is acquired after the linear transformation utilizing the synchronous reference rotating frame as per Equation (2). However, in order to calculate the active and reactive power of the grid in the form of space vector is explained in Equation (3):

$$\begin{aligned} V_{id} &= Ri_d + L\frac{di_d}{dt} + V_{gd} \\ V_{iq} &= Ri_q + L\frac{di_q}{dt} + V_{gq}, \end{aligned} \quad (2)$$

$$\begin{aligned} P &= 1.5 \times (V_{qd}I_q + V_{gd}I_d) \\ Q &= 1.5 \times (V_{qd}I_d - V_{gd}I_q), \end{aligned} \quad (3)$$

where (V_{qd}, I_q) and (V_{gd}, I_d) represent the *q* and *d* axis of voltage and current in the *d*–*q* synchronous reference frame at the grid side. As stated above, the system must operate at a power factor mostly near to 1 in ordinary operating mode. Accordingly, no reactive power is injected to the grid; thus by neglecting power losses, V_{qd} is zero, the formula in Equation (3) thereby converted as follows:

$$P = 1.5\left(V_{gd}I_d\right) \text{ and } Q = -1.5\left(V_{gd}I_q\right). \quad (4)$$

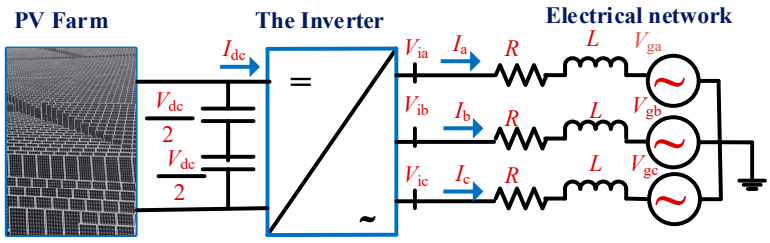

Figure 4. Three-phase (3-ph) view of the grid-connected voltage source inverter.

The decoupling control is realized for the active and reactive power of the proposed GCPS as indicated by Equation (4). The active and reactive powers are affected by I_d and I_q, respectively; therefore any adjustment of I_d and I_q can manage the active output power and reactive output power independently. Therefore, this strategy controlled the reactive power injection during the sag problem to achieve the required injection of active and reactive power according to the standard requirements.

In this study, the large-scale PV array generates a rated power of 5000 kW connected to the medium voltage side (11 kV) was designed. The current-controlled PV inverter was used in this design due to its ability to enhance the power factor and reduce the harmonic current distortion. A feed-forward decoupling PI current controller-based synchronous rotating reference frame (*d–q* control) was used to control the connection of the PV system to the grid. The inverter controller adopts double loops control mode including inner current loop (active current (I_d) and reactive current (I_q)) and outer voltage loop. The outer loop was utilized to stabilize or manage the DC-link voltage (V_{dc}). The injected active and reactive current components into the utility grid were controlled using PWM strategies. For synchronization, the phase-locked loop (PLL) based on (*d–q*) synchronous reference frame (SRF-PLL) was applied (see Figure 5) to lock the grid frequency and to support the reference synchronization signal for the inverter control system. It detected the phase angle and created an error signal by comparing the reference signal with the output signal. The loop filter eliminated unwanted harmonics from the error signal, while the voltage-controlled oscillator (VCO) in turn generated the output signal whose frequency varies around the system frequency depending on the output of the filter. Finally, the large-scale PVPP was connected to the distribution side of the grid through a step-up transformer (0.4–11) kV.

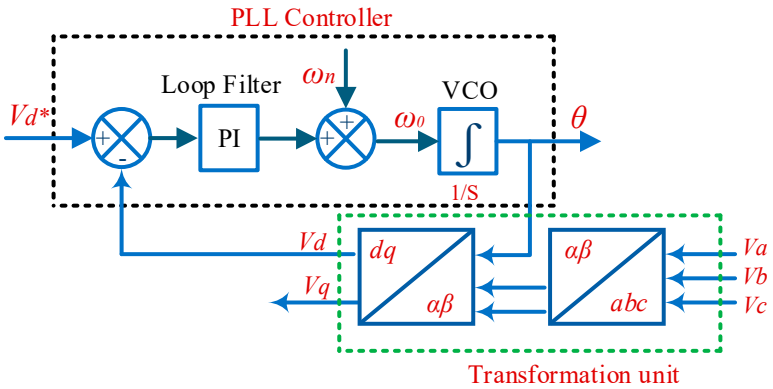

Figure 5. Phase-locked loop synchronous reference frame (SRF-PLL).

4. Compliance Strategies for Achieving Power Quality Requirements

The GCPS needs to manage and comply with the recent requirements concerning the voltage flicker, voltage sag, harmonics, voltage unbalance, frequency, and power factor toward grid stability. Accordingly, the power quality standard requirements compliance verification has to be done applied for the PVPP to confirm verification and compliance with the recent integration regulation disused above.

In this context, this section provides a power quality assessment and management of the large-scale PVPP connected to the distribution grid following the recent power quality technical regulations.

4.1. LVRT Capability Control for Voltage Sag Mitigation

The large cost associated with voltage sags can justify the use of sag mitigation strategies. In the literature, different methods had already used to mitigate the sag problems, for instance, a dynamic reactive compensation including static synchronous compensator (STATCOM) and the static VAR compensator. STATCOM devices utilize synchronous voltage sources in order to generate or absorb reactive power. The STATCOM is connected to the ac system via an interface transformer [16]. An SVC can mitigate the voltage sag and support the grid voltage by injecting the loads by the reactive current, which has been tested in [43]. Other techniques used to mitigate the sag events in the power system are the uninterruptible power supply and energy storage devices, which depend on the reactive current to mitigate the sag events [44]. Overall, all these techniques are expensive and increase system complexity. Therefore, the LVRT capability control using the inverter controller modification would be present in this study without any extra devices to achieve the recent requirements described in Section 2.1. This strategy can help in solving the sag problems towards grid stability.

The main feature of the proposed controller is that, once sag happens and causes the voltage to fall under 90%, the inverter has to switch from its normal operation mode to LVRT operation mode. To do this, it is essential to have a fast and precise sag detection unit. Therefore, the root means square (RMS) detection strategy is utilized to sense the voltage sag in the proposed LVRT control. This strategy is simple without any extra hardware or additional transformation. It basically tracks the RMS values of the d and q voltage components. The RMS detection method can compute the instant voltage of the grid (V_{ig}) as follows:

$$\begin{aligned} P &= 1.5\left(V_{gd}I_d\right) \\ Q &= -1.5\left(V_{gd}I_q\right). \end{aligned} \tag{5}$$

Here the V_{gd} denotes the active (d)-components of the grid voltage. According to the proposed control, once the sag is detected by the detection unit, the inverter has to switch its operation to the LVRT mode (see Figure 6) in which reactive current is injected to support the grid and voltage recovery. It is important to mention that the amount of reactive current that should be injected to the grid during sag incident depends on the sag depth as imposed by the requirements illustrated in Figure 2. For instance, if the sag happened and caused the voltage to decrease within the range from 90% to 50% from its nominal value, the amounts of injected reactive current should be calculated as per Equation (6). Otherwise, in case the voltage decreased less than 50% from its nominal value, 100% of the reactive current must be injected to mitigate the voltage sag. It is well-known that, in normal operation mode, the PVPPs have to operate at unity power factor. Therefore the reactive current becomes zero and the reactive power will be zero accordingly. However, to achieve the LVRT requirements, once the sag happened, the reactive current is injected based on the sag depth. In this context, the amount of maximum active current (I_d) injected to the grid is estimated according to Equation (7) in which the amount of active and reactive current not exceeding 110% of the inverter rated current (I_n) following to Equation (8).

$$I_q = \left(-2\frac{V_{ig}}{V_{\text{nominal}}} + 2\right) \times I_n. \tag{6}$$

$$I_d = \sqrt{1 - I_q^2} \times I_n. \tag{7}$$

$$\sqrt{I_q^2 + I_d^2} \leq (1.1 \times I_n). \tag{8}$$

As a result, the active and reactive power during sag is changed accordingly. However, to inject the reactive power and contribute to sag mitigation, it is important to ensure the inverter connectivity and protect against DC-overvoltage and ac-overcurrent during a fault. For this purpose, the proposed

controller used the crowbar [45] and the current limiter [46] to protect the inverter and other devices during the faults period.

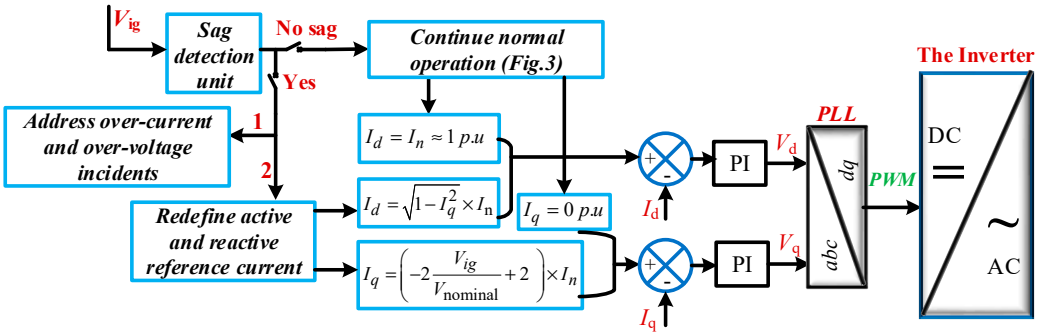

Figure 6. Schematic diagram of the proposed LVRT control strategy for sag mitigation.

4.2. Voltage Flicker Management

With a view to check compliance of the relevant standards described above, the P_{lt} and P_{st} are the best relevant flicker assessment that has been carried out on the proposed large-scale grid-connected PVPP model. In order to guarantee a less voltage fluctuation, flicker, and unbalance towards voltage stability, the dynamic voltage regulator (DVR) shown in Figure 7 was proposed. The DVR made-up of the DC energy source, IGBT inverter, and injection transformer (T_2) joined the transmission line in a series way. It is installed between the step-up transformer (T_1) and the interconnection point or PCC. The DVR has the ability to inject voltage to the system and thus bring the voltage to return its nominal operation to overcome the variance and flicker. DVR not only mitigated the voltage flicker and fluctuation but also mitigated the voltage unbalance and thus increased the grid stability [47].

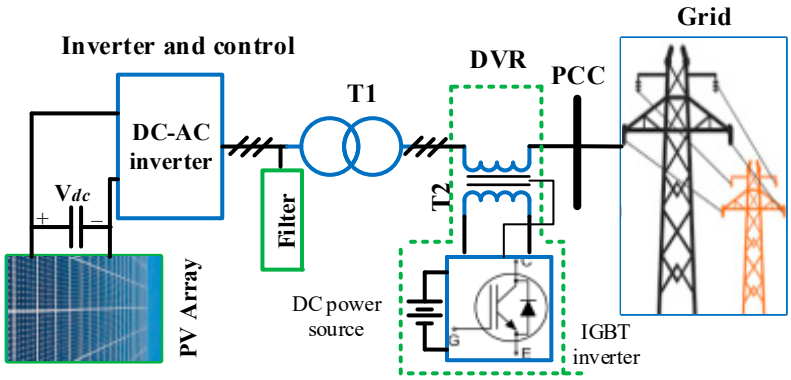

Figure 7. Grid-connected PV systems (GCPS) with a dynamic voltage regulator.

The simplified DVR power circuit is shown in Figure 8. It is exemplified by an ideal voltage source (V_{CNO}.) connected seriously between the PCC side (V_{pcc}) and supply (V_s). The X_{DVR} is defined as the reactance of the injection transformer and the filters. The R_{DVR} represents the DVR losses. These two values depend on the power rating (S_{DVR}) and voltage rating (V_{DVR}) of the DVR as expressed in Equations (9)–(12). Equation (13) represents the current (i_{DVR}) and voltage (v_{DVR}) handling capability of the DVR.

$$R_{DVR} = \frac{V_{DVR}^2}{S_{DVR}} \times v_{DVR,R}. \tag{9}$$

$$X_{DVR} = \frac{V_{DVR}^2}{S_{DVR}} \times v_{DVR,X}. \tag{10}$$

$$Z_{DVR} = \frac{V_{DVR}^2}{S_{DVR}} \times v_{DVR,Z}. \tag{11}$$

$$v_{DVR,Z} = v_{DVR,R} + jv_{DVR,X}. \tag{12}$$

$$(i_{DVR})\% = \frac{I_{DVR}}{I_{pcc,rated}} \times 100\% \text{ and } (v_{DVR})\% = \frac{V_{DVR}}{V_{s,rated}} \times 100\%. \tag{13}$$

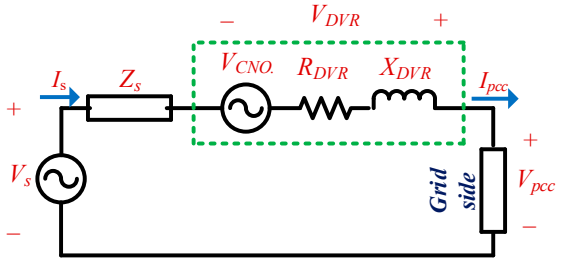

Figure 8. The simplified dynamic voltage regulator (DVR) model.

The proposed DVR can address the flicker incident using the three-phase voltage source inverter by injecting voltages in sequence into the power line at PCC. Thus, the voltage has measured at the PCC and connected to the digital flicker meter to calculate the flicker severity. The simulation was run for more than two hours to fulfill the GCs and standards requirements, which strictly require over a 600 s (10 min) period and 7200 s (2 h) period to measure the P_{st} and P_{lt}, respectively [29,48]. In order to assess the DVR ability to reduce the flicker severity at the PCC of PVPP connected MV of the grid side, a flicker meter has been developed. The assessment is done based on a statistical analysis approach inside the flicker meter. It computes the flicker levels that exceed 0.1% (P0.1 s), 1% (P1 s), 3% (P3 s), 10% (P10 s), and 50% (P50 s), respectively within the observation period. Then computes P_{st} and P_{lt}, flicker severity and shows the cumulative probability function. The overall system in the case of DVR operation is shown in Figure 9. The simulation data are added in Appendix A.

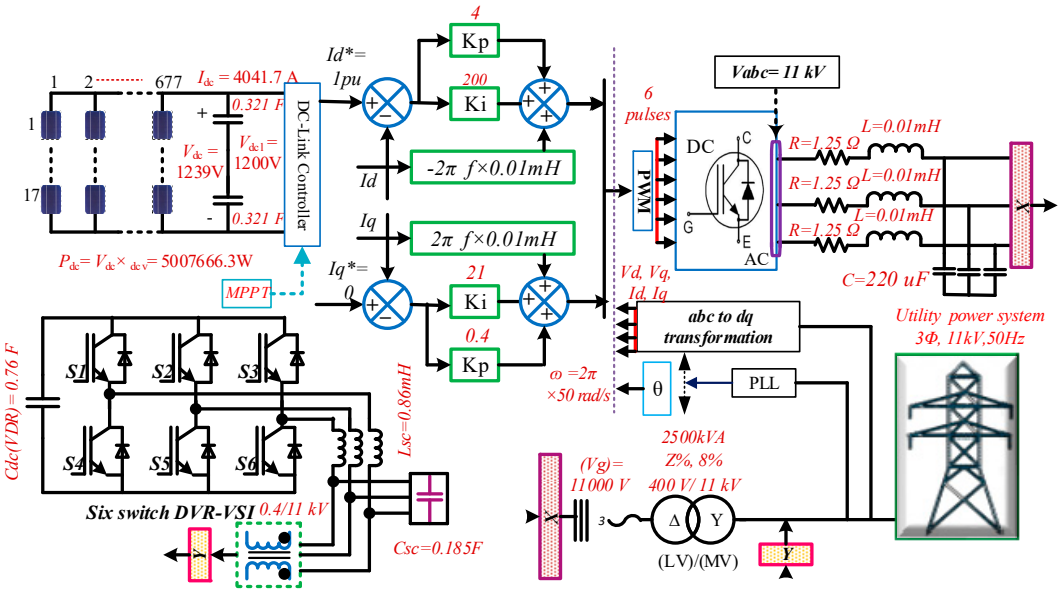

Figure 9. An overall system with DVR operation.

4.3. Harmonics Reduction According to the Standards Requirements

The structure and control approaches of GCPS can affect the harmonics level either positively or negatively. Therefore, GCPS stations should be designed carefully to achieve the recent standard requirements. In this study, the large-scale GCPS is connected to the MV side (11 kV), as described in Section 3. According to the harmonic standards (Tables 2 and 3), it is suggested that the total THD at the PCC should be less than 5% either for current total harmonics distortion (I_{THD}) or voltage total harmonics distortion (V_{THD}) expect UK standards, which need the I_{THD} to be less than 3%. In this study, the fast Fourier transform (FFT) Simulink tool was utilized to record the individual harmonics and then compute the THD of the PVPP output waveforms (current and voltage) at PCC.

In order to reduce the harmonics, the following criteria and strategies have been considered in the design procedure including (a) the self-commutated PV inverter is designed to mitigate the harmonics distortion; (b) single-stage conversion of the GCPS without DC–DC converter is utilized to decrease the output current and voltage harmonics; (c) the current-controlled PV inverter is designed for fast response compare to voltage-controlled inverter; and (d) sinusoidal PWM switching is considered for harmonics reduction, respectively. However, the current and voltage harmonics were oscillating at around 22.22% and 6.72%, respectively, which exceed the standards limits. Therefore, an appropriate RLC filter is designed while the PWM carrier frequency is increased to reduce the harmonic level.

4.4. Voltage Unbalance Assessment

In most cases, the voltage is balanced at the generation side; however, at the customer's level, the voltage may turn out to be unbalanced because of the improper distribution of the single-phase loads or uneven impedance of the system [49]. In this paper, the management and assessment of the voltage unbalance was carried out at the PCC to make sure that the injected voltage to the distribution system was well-balanced. Although the DVR was utilized to mitigate the fluctuation and flicker, it had a high ability to compensate for the voltage unbalance as well. The SRF-PLL was used to detect the voltage unbalance and reference voltage of the DVR using *abc* to *dq* transformation [20]. The voltage phage angle in the balanced situation was stored as a reference phase. Then afterward, the reference RMS voltage of the grid (V^*_{rms}) and the phase reference acquired (θ^*) were utilized to define the reference grid voltages values in the SRF based on Equations (14)–(16).

$$\theta^* = \arctan\frac{V_{dg,dc}}{V_{qg,dc}}. \tag{14}$$

$$V^*_{dg} = \sqrt{2} \times V^*_{rms} \times \sin(\theta^*). \tag{15}$$

$$V^*_{qg} = \sqrt{2} \times V^*_{rms} \times \cos(\theta^*). \tag{16}$$

The online comparison was performed between the line-to-neutral voltages of the grid (in *dq*) and the reference line-neutral grid voltages (in *abc*). In case any differences, the unbalance happened accordingly. The differences were therefore taken seriously as the *dq* values of the required DVR injected voltages as follows:

$$V^*_{DVR,d} = V^*_{dg} - V_{dg}, \tag{17}$$

$$V^*_{DVR,q} = V^*_{qg} - V_{qg}, \tag{18}$$

$$V^*_{DVR,0} = 0 - V_{0g}, \tag{19}$$

here $V^*_{DVR,d}$, $V^*_{DVR,q}$, and $V^*_{DVR,0}$ are the *d*, *q*, and zero components reference values in the SRF-PLL of the required DVR injected voltages, respectively. These values were transferred to *abc* system coordination, and consequently, the DVR reference voltage was obtained to minimize unbalance and fluctuation of the voltage at PCC to minimum levels.

5. Results and Discussion

5.1. Large-Scale Grid Connected PVPP

The large-scale GCPS simulation model was developed using MATLAB/Simulink 2019a environment. The rated power of this large-scale PV system was 5000 kW. The PV array consisted of 11,495 modules; each had rated 435 W of power distributes as 17 series modules connected in 677 parallel strings. The PV generators output voltage, V_o = 1239 V, output current, I_o = 4041.7 A, open-circuit voltage, V_{oc} = 1455.2 V, short circuit current, I_{sh} = 4355.14 A, and DC generated power, P_{out} = 5 MW, respectively. It is important to mention that these values were achieved at standard test conditions (STC), irradiation (G) = 1000 W/m^2, and temperature (T) = 25 °C.

The large scale PVPP was linked to the grid side through step-up transformer (0.4–11 kV), so that connected to a bus-bar at 11 kV substation. The output of DC voltage and current, line voltage of the inverter, ac voltage, ac current, and ac active and reactive output power at the PCC is shown in Figure 10. In this study, at PCC, the power quality assessment must be compatible with the recent integration standards and requirements.

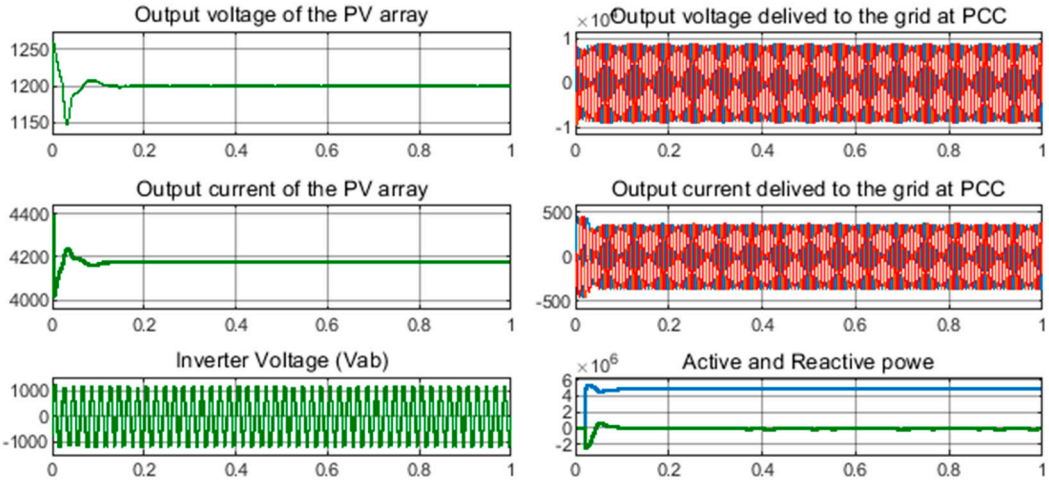

Figure 10. The output of the large scale grid-connected PV power plant.

5.2. Verification of the Compliance of Power Quality Requirements

The effectiveness of the control approaches and strategies used to meet the recent integration requirements were verified through the simulation results. Figure 11 shows the effectiveness of the proposed LVRT strategy to attain the LVRT requirements during voltage sag. It can be seen that, to validate the proposed LVRT technique, a three-phase voltage sag (the worst situation incident) occurs at the distribution side of the grid, which lasted for 0.15 s. It caused the PCC voltage to drop to 60% of its nominal value. Therefore, during fault time (0.45–0.6 s), the inverter should ride-through the fault and stay in the connection mode by addressing over-voltage and overcurrent. Furthermore, based on the requirement of the standards (Figure 2 and Equations (6) and (7)), the PV system had to provide the grid with an amount of reactive and active current equal to 0.2 pu and 0.8 pu, respectively. These values did not exceed the rated current of 1 pu in a balanced system and 1.1 as rated value. Hence, all conditions at fault period were stable so that the inverter could withstand the fault and inject the required amount of reactive power and thus support the voltage recovery. Once the fault was cleared, active current, reactive current, and other values were backed to pre-fault values. It could be concluded that the proposed control effectively overcame the disturbances, kept the inverter connected and ride-through the grid faults safely, and then injected the required amount of active and reactive power. It is important to mention that the fast and precise fault detection and protection from over-current as

a result of the fault using DC-chopper strategy played an important to achieve the required results, as stated by GCs.

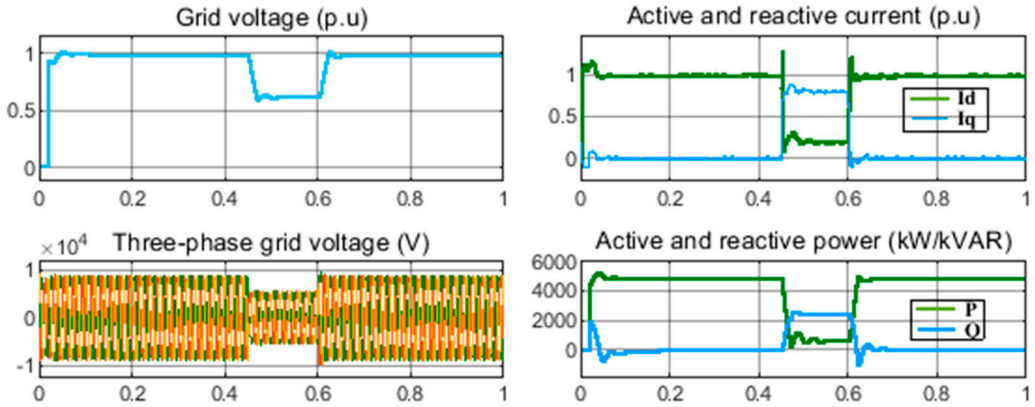

Figure 11. Simulation results of an LVRT control strategy with symmetrical 3-phase fault when the voltage dropped by 40% from its nominal voltage (voltage sag 60%) for 150 ms.

In order to measure the flicker severity, the digital flicker meter was run according to the requirements as mentioned above. Again in order to assess the DVR ability to reduce the flicker severity, the P_{st} and P_{lt} at the PCC is computed at 0.1% (P0.1 s), 1% (P1 s), 3% (P3 s), 10% (P10 s), and 50% (P50 s) within the observation and shows the cumulative probability function as shown in Figure 12. It is observed that the P_{st} and P_{lt} at the PCC were 0.43 pu and 0.18 pu, respectively, which are below the standards values stated in Table 1. These analysis results show the effectiveness of the proposed strategy to reduce the voltage flicker according to the recent integration requirements.

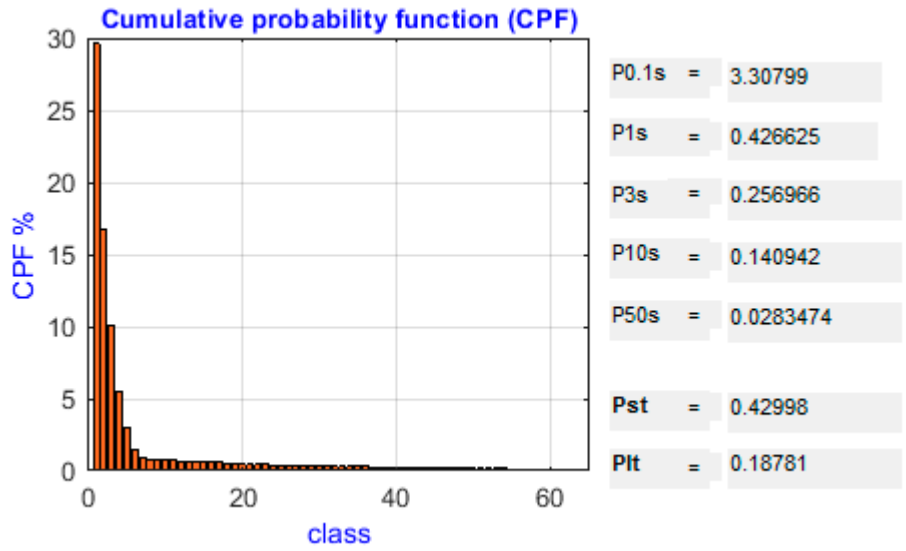

Figure 12. Long- and short-term flicker severity assessments and calculation.

For harmonics reduction, although the system was designed using proper control strategies and equipment; however, the I_{THD} and V_{THD} were still higher than the standard limit as shown in Figures 13 and 14, respectively. It can be seen that the harmonics of current and voltage waveforms were oscillating at 22.22% and 6.72%, respectively. Therefore, with the efficient design of RLC filter and increasing the switching frequency, the effectiveness of the proposed system was improved in which the I_{THD} was reduced to 0.97% and V_{THD} was minimized to 1.13% as shown in Figures 15 and 16, respectively.

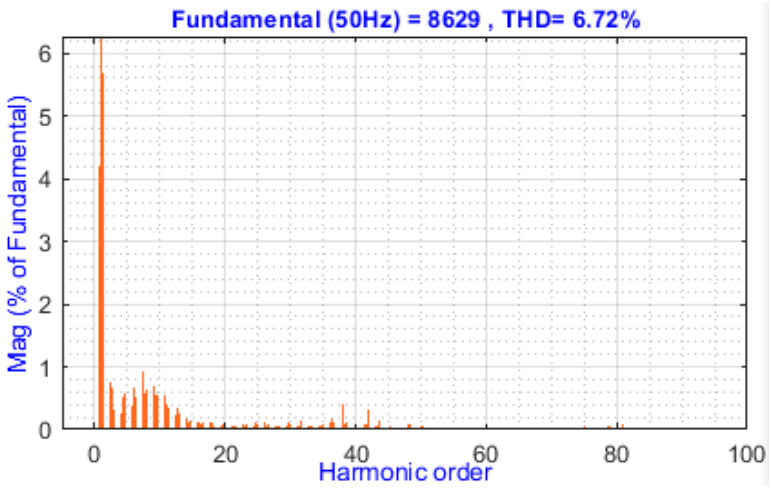

Figure 13. Total and individual harmonics levels of the output voltage at the point of common coupling (PCC).

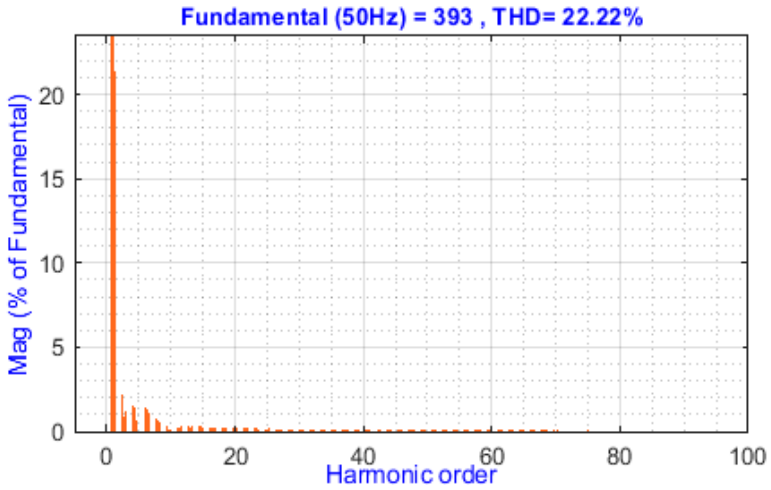

Figure 14. Total and individual harmonics levels of the output current at PCC.

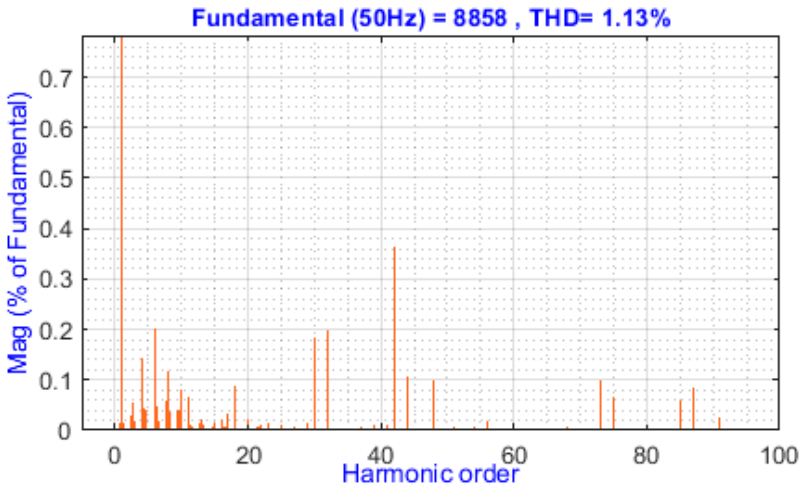

Figure 15. Total and individual harmonics level of the output voltage at PCC after filtering.

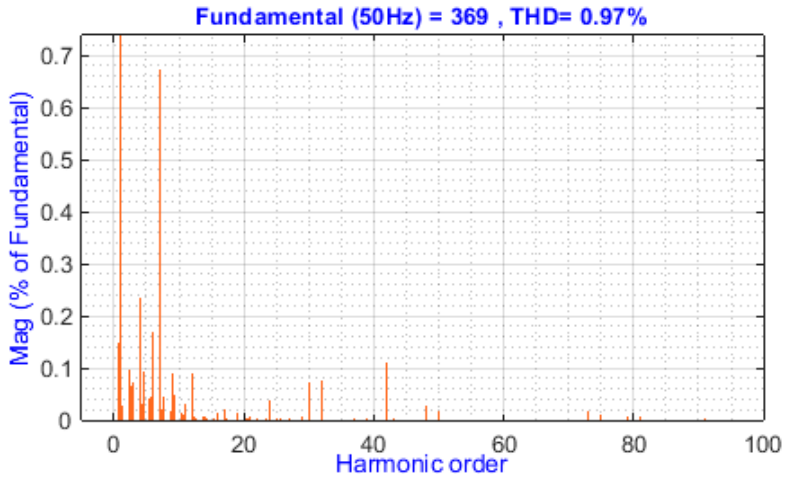

Figure 16. Total and individual harmonics level of the output current at PCC after filtering.

To test the harmonics distortion at PCC under different levels of solar irradiation, the irradiation decreased from STC (1000 W/m^2) into 600 W/m^2. It can be seen that the V_{THD} and I_{THD} values at the PCC were under the limits of the standard as shown in Figures 17 and 18, respectively. However, when the irradiation was 600 W/m^2, the harmonic distortions increased to 1.29% and 1.82% from that of 1.13% and 0.97%, respectively of 1000 W/m^2. This happened because the harmonics tend to rise once the modulation index decreases; however, the harmonics level is minimum with the modulation index tending to be 1. Therefore, the relation between the harmonics and irradiation is a contrary relationship so that the PVPP operates at low irradiation could inject more harmonics to the grid.

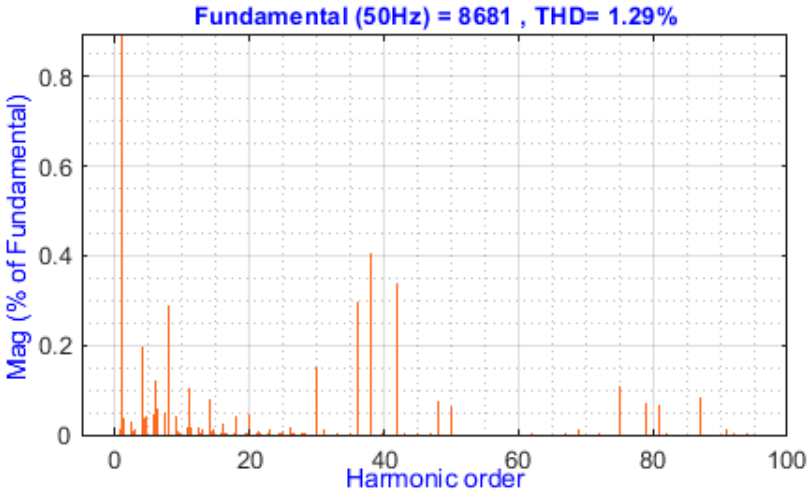

Figure 17. Total and individual harmonics level of the output voltage at PCC after filtering with low solar irradiation (600 W/m^2).

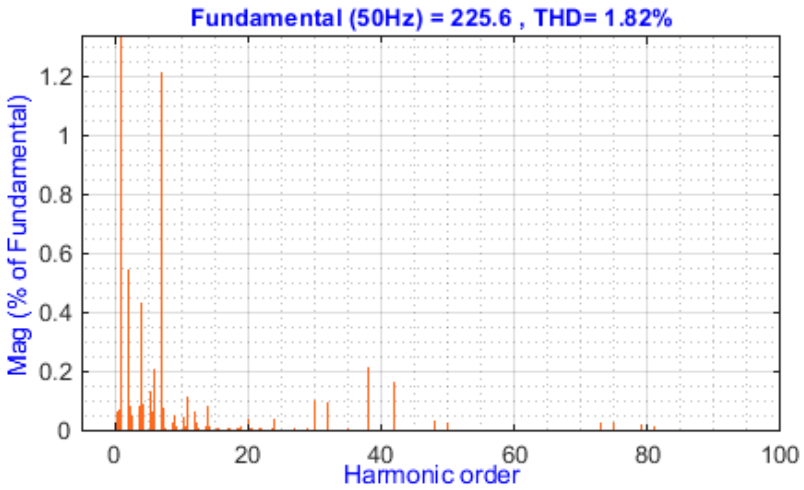

Figure 18. Total and individual harmonics level of the output current at PCC after filtering with low solar irradiation (600 W/m^2).

Regarding voltage unbalance, all requirements need the VUF to remain at least under 2%. The VUF test was conducted to measure the unbalance level at the PCC including DVR connection. The effectiveness of the DVR to enhance the voltage profile, the obtained results in Figure 19 shows that the VUF fulfilled the recent requirements in mitigating voltage unbalance profile. At all the time the unbalance still was within the minimum limits.

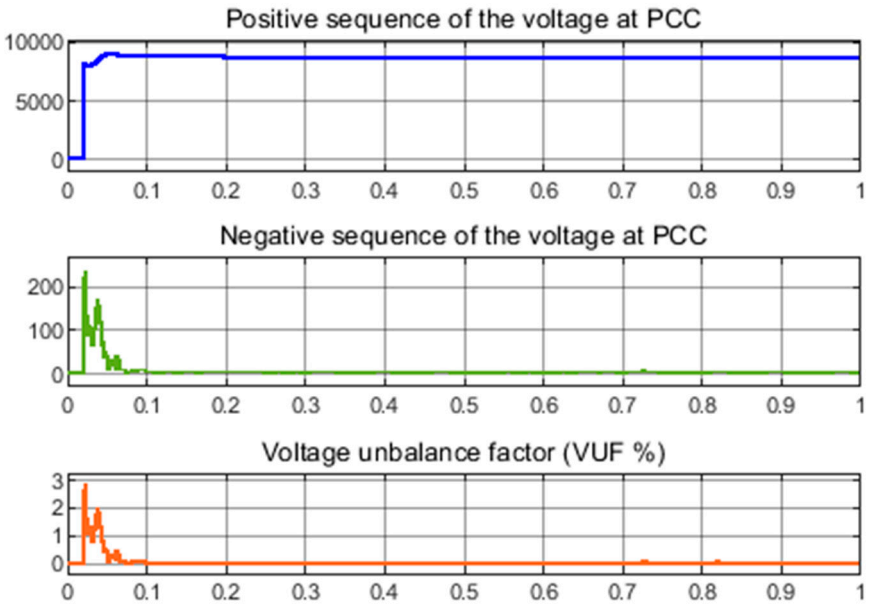

Figure 19. Voltage unbalance factor (VUF%) at the PCC.

The frequency variation is a serious power quality issue due to its high effect on power system stability, reliability, and quality. Thus, during the normal and abnormal operation, the level of frequency should stay within the ±1 Hz limit specified in the standards. In order to test the frequency fluctuation performance for the proposed large-scale GCPS operating at 50 Hz, the symmetrical three-phase grid fault occurred at the distribution side of the utility grid. The fault duration was 0.1 s of 0.4 s simulation, which occurred between 0.15 and 0.25 s. The obtained results show that the frequency dynamics stayed within the required limits even during the period of disturbances as shown in Figure 20.

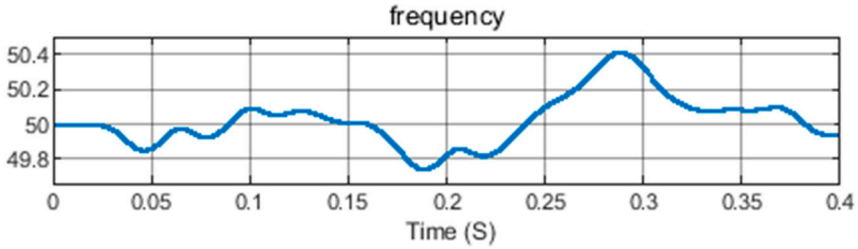

Figure 20. Dynamics response of the system frequency.

Most of the PV inverters are designed for grid-connected services operating near to the unity power factor (PF) in the normal operation; this is because the reactive power reference is kept at zero. Figure 21 shows the behavior of PF is near to unity PF, which matches the technical standards requirements presented in Table 4, i.e., leading or lagging PF not less than 0.85 pu.

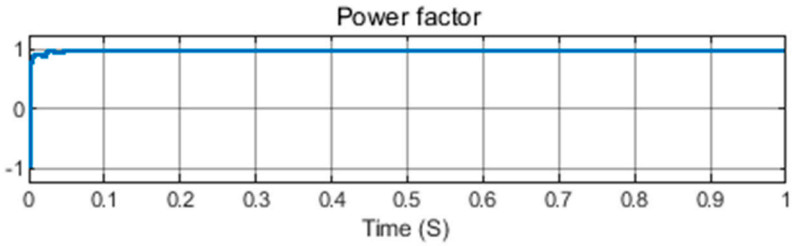

Figure 21. The power factor of the photovoltaic power plant (PVPP) at rated inverter output power.

5.3. Comparison between Proposed and Existing Methods

This section introduces the consistency of the above results with other previous studies introduced in the literature. Some studies have been used energy storage devices for the GCPSs to meet the LVRT requirements [19]. Although these methods fulfilled the LVRT to some extent, this strategy is hard to be extensively applied in the industry because of the high investment price and short life cycle of energy storage units. Additionally, high fluctuation and overshooting appeared before and after the sag event. When comparing the proposed control strategy with the study introduced in [17] that used the coordination between the PV system inverter and the STATCOM to enhance the LVR capability. It can be noticed that it injected the required reactive current to support the voltage recovery during the fault. Although STATCOM is effective in injecting reactive current according to the LVRT requirements, this method has not addressed the over-voltage incident during sag time. Besides, it increases the complexity and cost due to adding external hardware to the system and does not deal with inverter protection. Some studies were introduced to manage the PQ issues such as voltage harmonics [50], current harmonics [32], flicker problem [23], and voltage unbalance [21] in order to meet the recent requirements concerning the PV penetration at the PCC. By comparing the results of these strategies with the proposed method, in most cases, the proposed method was better. In sum, the presented results were compatible with the recent requirements, which is an important indicator of the results' verification. In addition, as compared to existing methods described in Table 5, the proposed method effectively enhanced the PQ at the PCC and got an important enhancement with the possible low complexity and cost. Table 5 shows a comparison between the existing and proposed methods.

Table 5. Comparison table between the proposed and existing methods.

PQ Event	Method	Ref.	Fulfillment of the Standards	Limitation of the Method	Proposed Method
LVRT	Energy storage system	[19]	Yes. Grid is supported by reactive power.	High fluctuation and overshooting; High investment price and short lifestyles cycle; Increase the complexity; Require regular inspection and maintenance	Injected required reactive current; Protect inverter during sag event; Addressed excessive DC voltage.
LVRT	STATCOM and SVC	[16,17]	Inject reactive currents and enhance FRT capability	Increase the complexity and cost; Did not address the increasing of DC-link voltage during grid faults; Do not dealt on inverter protection	No extra hardware; Modified inverter controller; Lower cost; Less complexity.
THDV	New inverter configuration	[50]	3.24%	Higher voltage THD than the proposed method	1.13%.
THDI	Active power filter	[32]	3.46%	Higher current THD than the proposed method	0.97
Flicker	Novel estimation method	[23]	P_{st} = 0.72 P_{lt} = 0.16	Better than the proposed method with respect to P_{lt}, however; for P_{st}, the proposed method is better	P_{st} = 0.42 P_{lt} = 0.18
Voltage Unbalance	Dynamic voltage stability control strategy	[21]	VUF% = 2.85 case 3	The proposed method generated better results.	VUF% = 0.6

6. Conclusions

This paper presented the power quality assessment and management of single-stage three-phase PVPP connected to the MV side of the electrical grid. The recent power quality integration requirements and standards concerning voltage sag, voltage flicker, harmonics, voltage unbalance frequency, and power factor were fully considered. The simulation results showed that all these power quality issues were modified and degraded to the standard defined level using efficient controls and compliance strategies. The voltage sag was mitigated by the injection of reactive current using modified inverter LVRT capability control. This control was developed based on the modification of traditional inverter control to operate in two modes of operations, which are normal and faulty (LVRT) operation modes during a sag event. The controller can be transferred rapidly and precisely between two modes using the RMS detection method DVR showed its ability to enhance the voltage stability by addressing the voltage flicker and unbalance. The proper control strategies and RLC filter were designed to reduce the voltage and current harmonics as verified by the obtained results. It was observed that the PVPP operated at low irradiation could inject more harmonics to the grid. Long and short flicker, voltage unbalance, voltage, and current harmonics are 0.42 pu, 0.18 pu, 0.6%, 1.3%, and 0.97%, respectively, which did not violate the standard requirements. In sum, the fulfillment of the standards at the connection point between the PVPP and the main grid will assure that no bad quality of the generated power will be injected into the power system and then increase the system security and stability. This study will potentially be a foundation for the power system operators, developer of PV systems, and manufacturers with regard to the future compliance verification of the recent interconnection regulations.

Author Contributions: Conceptualization, A.Q.A.-S., M.A.H., and A.A.A.; Methodology, A.Q.A.-S., M.A.H. and K.P.J.; Simulation, A.Q.A.-S.; Validation M.A.H., and A.A.A.; Resources, A.A.A., K.P.J. and A.E.P.A.; Project Administration, M.A.H. and K.P.J.; Writing—original draft, A.Q.A.-S., A.A.A.; Writing—review and editing, A.Q.A.-S., M.A.H., K.P.J., A.A.A., and A.E.P.A.; Supervision, M.A.H. All authors have read and agreed to the published version of the manuscript.

Funding: This research received funded by the Ministry of Higher Education, Malaysia under Universiti Tenaga Nasional using grant no. 20190101LRGS and UNITEN Bold Strategic funding grant 10436494/B/2019093.

Conflicts of Interest: Authors declare no conflict of interest.

Appendix A. System Parameters of PV Farm

PV system: Maximum power of each PV module (P_{max}) = 435 kW, Numbers of PV array modules (N_{pv}) = 11,509, numbers array strings (N_{PVp}) = 677, numbers of the series modules (V_{PVs}) = 17, ideally factor of the diode (m) = 1.02, output current (I_{dc}) = 4041.7 A, output voltage (V_{dc}) = 1239 V, DC output power (P_{dc}) = 5000 kW, open circuit voltage (V_{oc}), short circuit current (I_{sh}) = 1455.2 V, irradiation (G) = 1000 W/m^2, and temperature (T) = 25 °C.

System, controls, and grid Parameters: voltage of the DC-link (V_{dcl}) = 1200 V, capacitor of DC-link (C_{dc}) = 0.321 F, grid frequency (ω) = 2π*50 rad/s, switching frequency (f) = 2 kHz, filter resistance (R) = 1.25 Ω, filter inductance (L) = 0.01 mH, filter capacitance (C) = 220 uF, parameters of PI current loop K_p = 0.4, K_i = 21, parameters of PI voltage loop K_p = 4, K_i = 200, parameters of PI in PLL K_p = 0.0027, K_i = 1.113, Grid voltage (V_g) = 11 kV, grid current (I_g) = 454.5 A, output ac power (P_{ac}) = 491.3 kW, Δ-Y transformer = 0.4/11 kV. Switching frequency of DVR (f_{sw}) = 10 kHz, DC voltage of DVR = 800 V, DC-link capacitor of DVR ($Cdc_{(DVR)}$) = 0.76 F, LC filter of the DVR are 0.86 mH and 0.185 F, respectively.

References

1. Global Status Report. Renewables 2019 Global Status Report-REN21. Available online: https://www.unenvironment.org/resources/report/renewables-2019-global-status-report (accessed on 22 June 2019).
2. Di Silvestre, M.L.; Favuzza, S.; Sanseverino, E.R.; Zizzo, G.; Ngoc, T.N.; Pham, M.-H.; Nguyen, T.G. Technical rules for connecting PV systems to the distribution grid: a critical comparison of the Italian and Vietnamese frameworks. In Proceedings of the 2018 IEEE International Conference on Environment and Electrical Engineering and 2018 IEEE Industrial and Commercial Power Systems Europe (EEEIC/I&CPS Europe), Palermo, Italy, 12–15 June 2018; pp. 1–5.
3. Troester, E. New German grid codes for connecting PV systems to the medium voltage power grid. In Proceedings of the 2nd International Workshop on Concentrating Photovoltaic Power Plants: Optical Design, Production, Grid Connection, Lisbon, Portougal, 12–13 November 2009; pp. 9–10.
4. CEI-Comitato Elettrotecnico Italiano. Reference Technical Rules for the Connection of Active and Passive Consumers to the HV and MV Electrical Networks of Distribution Company. Available online: http://www.ceiweb.it/ (accessed on 23 August 2019).
5. Federal Energy Regulatory Commission (FERC). *156 FERC ¶ 61,182: Order on Proposed Tariff Revisions*; FERC: Washington, DC, USA, 2016.
6. Australian Energy Market Commission (AEMC). National Electricity Rules Version 80. Available online: http://www.aemc.gov.au/Energy-Rules/National-electricity-rules/Rules/National-Electricity-Rules-Version-80 (accessed on 12 January 2019).
7. Stone, G.; Stranges, M.K.; Dunn, D.G. Common questions on partial discharge testing: A review of recent developments in IEEE and IEC standards for offline and online testing of motor and generator stator windings. *IEEE Ind. Appl. Mag.* **2015**, *22*, 14–19. [CrossRef]
8. IEEE Committee. *IEEE Standard for Interconnecting Distributed Resources with Electric Power Systems1547*; Institute of Electrical and Electronics Engineers: New York, NY, USA, 2014. [CrossRef]
9. Al-Shetwi, A.Q.; Sujod, M.Z. Grid-connected photovoltaic power plants: A review of the recent integration requirements in modern grid codes. *Int. J. Energy Res.* **2018**, *42*, 1849–1865. [CrossRef]
10. Alshahrani, A.; Omer, S.; Su, Y.; Mohamed, E.; Alotaibi, S. The technical challenges facing the integration of small-scale and large-scale PV systems into the grid: A critical review. *Electronics* **2019**, *8*, 1443. [CrossRef]
11. Roberts, C. *Review of International Grid Codes*; Lawrence Berkeley National Laboratory: Berkeley, CA, USA, 2018.
12. Rodrigues, E.; Osório, G.; Godina, R.; Bizuayehu, A.; Lujano-Rojas, J.; Catalão, J. Grid code reinforcements for deeper renewable generation in insular energy systems. *Renew. Sustain. Energy Rev.* **2016**, *53*, 163–177. [CrossRef]
13. Honrubia-Escribano, A.; García-Sánchez, T.; Gómez-Lázaro, E.; Muljadi, E.; Molina-Garcia, A. Power quality surveys of photovoltaic power plants: Characterisation and analysis of grid-code requirements. *IET Renew. Power Gener.* **2015**, *9*, 466–473. [CrossRef]

14. Marinopoulos, A.; Papandrea, F.; Reza, M.; Norrga, S.; Spertino, F.; Napoli, R. Grid integration aspects of large solar PV installations: LVRT capability and reactive power/voltage support requirements. In Proceedings of the 2011 IEEE Trondheim PowerTech, Trondheim, Norway, 19–23 June 2011; pp. 1–8.
15. Hossain, E.; Tür, M.R.; Padmanaban, S.; Ay, S.; Khan, I. Analysis and mitigation of power quality issues in distributed generation systems using custom power devices. *IEEE Access* **2018**, *6*, 16816–16833. [CrossRef]
16. Popavath, L.; Kaliannan, P. Photovoltaic-STATCOM with low voltage ride through strategy and power quality enhancement in a grid integrated wind-PV system. *Electronics* **2018**, *7*, 51. [CrossRef]
17. Castilla, M.; Miret, J.; Camacho, A.; Matas, J.; de Vicuña, L.G. Voltage support control strategies for static synchronous compensators under unbalanced voltage sags. *IEEE Trans. Ind. Electron.* **2014**, *61*, 808–820. [CrossRef]
18. Movahedi, A.; Niasar, A.H.; Gharehpetian, G.B. LVRT improvement and transient stability enhancement of power systems based on renewable energy resources using the coordination of SSSC and PSSs controllers. *IET Renew. Power Gener.* **2019**, *13*, 1849–1860. [CrossRef]
19. Ota, J.I.Y.; Sato, T.; Akagi, H. Enhancement of performance availability and flexibility of a battery energy storage system based on a modular multilevel cascaded converter (MMCC-SSBC). *IEEE Trans. Power Electron.* **2016**, *31*, 2791–2799. [CrossRef]
20. Rohouma, W.; Balog, R.S.; Peerzada, A.A.; Begovic, M.M. D-STATCOM for a Distribution Network with Distributed PV Generation. In Proceedings of the 2018 International Conference on Photovoltaic Science and Technologies (PVCon), Ankara, Turkey, 4–6 July 2018; pp. 4849–4854.
21. Islam, M.; Mithulananthan, N.; Hossain, J.; Shah, R. Dynamic voltage stability of unbalanced distribution system with high penetration of single-phase PV units. *J. Eng.* **2019**, *2019*, 4074–4080. [CrossRef]
22. Tang, C.-Y.; Kao, L.-H.; Chen, Y.-M.; Ou, S.-Y. Dynamic power decoupling strategy for three-phase PV power systems under unbalanced grid voltages. *IEEE Trans. Sustain. Energy* **2018**, *10*, 540–548. [CrossRef]
23. Rahman, S.; Moghaddami, M.; Sarwat, A.I.; Olowu, T.; Jafaritalarposhti, M. Flicker estimation associated with PV integrated distribution network. In Proceedings of the SoutheastCon 2018, Tampa Bay, FL, USA, 19–22 April 2018; pp. 1–6.
24. Montoya, F.; Baños, R.; Alcayde, A.; Montoya, M.; Manzano-Agugliaro, F. Power quality: Scientific collaboration networks and research trends. *Energies* **2018**, *11*, 2067. [CrossRef]
25. Geng, Y.; Yang, K.; Lai, Z.; Zheng, P.; Liu, H.; Deng, R. A Novel Low Voltage Ride Through Control Method for Current Source Grid-Connected Photovoltaic Inverters. *IEEE Access* **2019**, *7*, 51735–51748. [CrossRef]
26. Islam, S.U.; Zeb, K.; Din, W.U.; Khan, I.; Ishfaq, M.; Hussain, A.; Busarello, T.D.C.; Kim, H.J. Design of robust fuzzy logic controller based on the levenberg marquardt algorithm and fault ride trough strategies for a grid-connected PV system. *Electronics* **2019**, *8*, 429. [CrossRef]
27. Tarafdar Hagh, M.; Khalili, T. A review of fault ride through of PV and wind renewable energies in grid codes. *Int. J. Energy Res.* **2019**, *43*, 1342–1356. [CrossRef]
28. Rey-Boué, A.B.; Guerrero-Rodríguez, N.; Stöckl, J.; Strasser, T.I. Modeling and design of the vector control for a three-phase single-stage grid-connected PV system with LVRT capability according to the Spanish grid code. *Energies* **2019**, *12*, 2899. [CrossRef]
29. Elshahed, M. Assessment of sudden voltage changes and flickering for a grid-connected photovoltaic plant. *Int. J. Renew. Energy Res.* **2016**, *6*, 1328–1335.
30. Silsüpür, M.; Türkay, B.E. Flicker source detection methods based on IEC 61000-4-15 and signal processing techniques—A review. *Balkan J. Electr. Comput. Eng.* **2015**, *3*, 93–97. [CrossRef]
31. Canadian Standards Association (CSA). Interconnection of Distributed Resources and Electricity Supply Systems, CSA C22.3 No. 9-08-R2015. Available online: https://www.csagroup.org/ (accessed on 14 August 2019).
32. Colque, J.C.; Azcue, J.L.; Ruppert, E. Photovoltaic system grid-connected with active power filter functions for mitigate current harmonics feeding nonlinear loads. In Proceedings of the 2018 13th IEEE International Conference on Industry Applications (INDUSCON), São Paulo, Brazil, 21–22 December 2018; pp. 208–214.
33. Memon, M.A.; Mekhilef, S.; Mubin, M.; Aamir, M. Selective harmonic elimination in inverters using bio-inspired intelligent algorithms for renewable energy conversion applications: A review. *Renew. Sustain. Energy Rev.* **2018**, *82*, 2235–2253. [CrossRef]
34. IEEE Std. *IEEE Recommended Practice for Utility Interface of Photovoltaic (PV) Systems*; IEEE, Ed.; IEEE Std: Piscataway, NJ, USA, 2003; pp. 929–2000.

35. Schwartfeger, L.; Santos-Martin, D. Review of distributed generation interconnection standards. In Proceedings of the EEA Conference & Exhibition, Auckland, New Zealand, 25–27 June 2019; pp. 18–20.
36. Bayliss, C.R.; Bayliss, C.; Hardy, B. *Transmission and Distribution Electrical Engineering*; Elsevier: Amsterdam, The Netherlands, 2012.
37. Kim, Y. Development and analysis of a sensitivity matrix of a three-phase voltage unbalance factor. *IEEE Trans. Power Syst.* **2018**, *33*, 3192–3195. [CrossRef]
38. Cleveland, F. IEC 61850-7-420 communications standard for distributed energy resources (DER). In Proceedings of the 2008 IEEE, Power and Energy Society General Meeting-Conversion and Delivery of Electrical Energy in the 21st Century, Pittsburgh, PA, USA, 20–24 July 2008; pp. 1–4.
39. Wu, Y.-K.; Lin, J.-H.; Lin, H.-J. Standards and guidelines for grid-connected photovoltaic generation systems: A review and comparison. *IEEE Trans. Ind. Appl.* **2017**, *53*, 3205–3216. [CrossRef]
40. GB/T. *Technical Rule for PV Power Station Connected to Power Grid*; Chinese Enterprise Standards; China National Standards: Beijing, China, 2012.
41. Ghassemi, F.; Perry, M. *Review of Voltage Unbalance Limit in the GB Grid Code CC. 6.1. 5 (b)*; National Grid Report; GB: Beijing, China, 2014.
42. Dreidy, M.; Mokhlis, H.; Mekhilef, S. Inertia response and frequency control techniques for renewable energy sources: A review. *Renew. Sustain. Energy Rev.* **2017**, *69*, 144–155. [CrossRef]
43. Hamdeen, I.; Saeed, M.A.; Badran, E.A. Voltage Dip's Mitigation during PV-Grid-Connection Using STATCOM. In Proceedings of the 2018 Twentieth International Middle East Power Systems Conference (MEPCON), Cairo, Egypt, 18–20 December 2018; pp. 760–766.
44. Khawla, E.M.; Chariag, D.E.; Sbita, L. A control strategy for a three-phase grid connected PV system under grid faults. *Electronics* **2019**, *8*, 906. [CrossRef]
45. Haidar, A.M.; Julai, N. An improved scheme for enhancing the ride-through capability of grid-connected photovoltaic systems towards meeting the recent grid codes requirements. *Energy Sustain. Dev.* **2019**, *50*, 38–49. [CrossRef]
46. Oon, K.H.; Tan, C.; Bakar, A.; Che, H.S.; Mokhlis, H.; Illias, H. Establishment of fault current characteristics for solar photovoltaic generator considering low voltage ride through and reactive current injection requirement. *Renew. Sustain. Energy Rev.* **2018**, *92*, 478–488. [CrossRef]
47. Bozalakov, D.; Laveyne, J.; Desmet, J.; Vandevelde, L. Overvoltage and voltage unbalance mitigation in areas with high penetration of renewable energy resources by using the modified three-phase damping control strategy. *Electr. Power Syst. Res.* **2019**, *168*, 283–294. [CrossRef]
48. Kopicka, M.; Ptacek, M.; Toman, P. Analysis of the power quality and the impact of photovoltaic power plant operation on low-voltage distribution network. In Proceedings of the 2014 Electric Power Quality and Supply Reliability Conference (PQ), Rakvere, Estonia, 11–13 June 2014; pp. 99–102.
49. Chen, T.-H.; Yang, C.-H.; Yang, N.-C. Examination of the definitions of voltage unbalance. *Int. J. Electr. Power Energy Syst.* **2013**, *49*, 380–385. [CrossRef]
50. Bhukya, M.N.; Kota, V.R.; Depuru, S.R. A simple, efficient, and novel standalone photovoltaic inverter configuration with reduced harmonic distortion. *IEEE Access* **2019**, *7*, 43831–43845. [CrossRef]